# Mechano-Electric Feedback Effects in a Ventricular Myocyte Model Subjected to Dynamic Changes in Mechanical Load

I Cenci[1,2], S Morotti[2], J Negroni[3], B Rodriguez[1], S Severi[2]

[1]Computing Laboratory, University of Oxford, Oxford, UK
[2]Biomedical Engineering Laboratory, University of Bologna, Cesena, Italy
[3]Department of Biology, Favaloro University, Buenos Aires, Argentina

## Abstract

*The effect of mechano-electric feedback (MEF) on myocyte's action potential (AP) has been largely studied considering constant stretches. The present study examined the role of MEF utilizing a model built by integrating mathematical descriptions of cardiac myocyte's electrical activity, contraction and MEF. This model simulates the four phases of the cardiac cycle as a sequence of isometric and isotonic contractions/relaxations, i.e. ideal work loops (WLs). Intracellular $Ca^{2+}$ controls contraction and sarcomere length is used as input to MEF, that in turn affects the AP through the action of stretch-modulated currents. Simulations were conducted to investigate the role of MEF in modulating electrical activity during WL for different length preloads and force afterloads. Results were in agreement with experimental WL and MEF studies. Moreover, on the base of simulation results, it can be asserted that the generation of arrhythmogenic phenomena could arise when the strength of the MEF is increased, as under heavy myocardium stress conditions.*

## 1. Introduction

The impact of mechanical events, changes in tension and force, and spatial displacement on the heart's electrical properties, namely the MEF, and its role in normal and pathological physiology has become an important chapter in contemporary cardiovascular biology [1].

The vast majority of research on MEF effect on single intact cardiomyocyte's AP has been conducted in mechanically unloaded cells or considering constant stretches [2]. This approach gives the possibility to simplify experimental protocols and, as a consequence, obtain reliable results. Model based analysis of experimental results is facilitated as well: given either a certain value of sarcomere stretch (or conductance of the stretch-modulated channels) it is possible to consider only the effect of MEF on the AP, without having to model how stretch is generated by the contracting myocyte at each time step.

The weak point of this approach is that simulated dynamics are really different from that of the real system during the cardiac cycle.

This study examined the role of MEF when cells undergo changes that are more similar to those of the in situ setting, in which sarcomere length varies following ideal WLs, obtained as a sequence of isometric and isotonic contractions/relaxations, and affects the stretch-modulated currents ($I_{ns}$ and $\Delta I_{k^+}$) in real time.

## 2. Methods

A model of mammalian myocyte contraction [3] was incorporated into a complete mathematical description of AP, ionic currents and $Ca^{2+}$ transient of the guinea pig ventricular cell [4]. In addition, the effect of myocyte's strain on stretch-modulated channels was implemented by integrating a modified version of the MEF model proposed by Gurev et al. [5].

As Figure 1 shows, the link between AP and contraction models was represented by intracellular $Ca^{2+}$ concentration ($[Ca^{2+}]_i$) while the contraction model provided half sarcomere length ($L_m$) and total muscle force ($F_m$) generated from $[Ca^{2+}]_i$ at every time step. By switching between contraction modes it was possible to reproduce the four phases of the cardiac cycle, i.e. a sequence of isometric and isotonic contractions/relaxations. Ideal WLs differ from real ones since they employ purely isotonic contractions (straight lines in the Force-Length diagram) instead of physiological quasi-isotonic ones, but this can be considered an acceptable approximation since they do not differ significantly from one another. In particular, the sequence of isometric and isotonic contractions/relaxations followed the setup implemented by Iribe et al. [6]:

- for phase 1 (isometric contraction) $L_m$ was kept equal to

a user-defined preload value until the time at which active force reached a user-defined afterload;
• for phase 2 (isotonic contraction) $L_m$ decreased in order to keep $F_m$ constant, until the time at which peak shortening was reached;
• for phase 3 (isometric relaxation) $F_m$ decreased due to the fading of the contraction and the phase ended when $F_m$ reached the initial resting value;
• for phase 4 (isotonic relaxation) $L_m$ increased in order to keep $F_m$ constant and reached the initial value, which implied the closure of the WL.

Once the WL was completed, a new cycle began in response to the subsequent pacing stimulus.

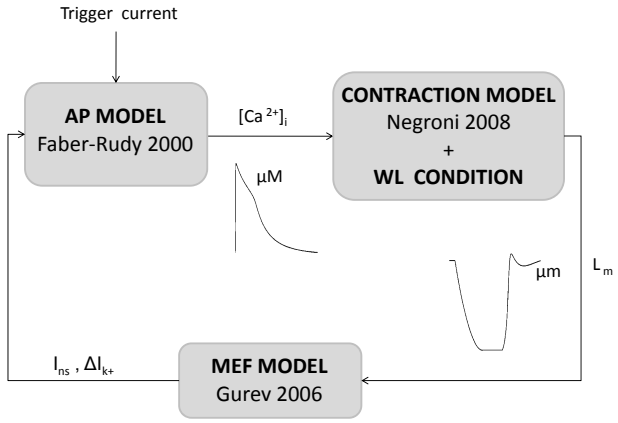


Figure 1. Schematic structure of the mathematical model.

The AP and contraction model parameters were the same as in [4][3], with the following modifications necessary to reproduce the experimental setup by Iribe et al. [6]: setting of the stimulation period to 500 ms; slight changes in bath ionic concentrations ($[Ca^{2+}]_o$=1.8 mM, $[Na^+]_o$=140 mM, $[K^+]_o$=5.4 mM); speedup by a factor of 1.5 of the chemical reaction constants ($Y_b$, $Z_b$, $f$, $Z_a$, $Y_p$, $Z_p$, $Y_r$, $Z_r$, $Y_d$) and the parameters $B_w$, $B_p$ involved in differential equations restoring velocity bridge elongation; change of the resting length of the parallel elastic element $L_o$ to 0.935 $\mu$m.

Moreover, $L_m$ linked together contraction and MEF models since stretch-modulated currents respond to a change in cellular stretch. Modifications made to the model by Gurev et al. consist in the addition to the equations of two parameters: membrane capacitance $C_m$ and cell area $A$. Values were 200 pF and 20000 $\mu m^2$, respectively. These additional parameters were necessary to make current unit coherent with that of our AP model and led to the following formulation:

$$I_{ns} = \frac{1}{10}\frac{1}{Cm}L(\lambda)[\gamma\rho A(V_m + 10)] \tag{1}$$

$$\Delta I_{k^+} = \frac{5.25}{5.09}\frac{1}{Cm}L(\lambda)\cdot [(I_{K1} + I_{Ko})_{(stretched)} - (I_{K1} + I_{Ko})_{(unstretched)}] \tag{2}$$

$$L(\lambda) = \frac{1}{1 + Ke^{-\alpha(\lambda-1)}} \tag{3}$$

The stretch ratio $\lambda$ was defined as ratio between current and resting half sarcomere length:

$$\lambda = \frac{L_m}{L_{m_o}} \tag{4}$$

In addition, we had to tune the balance of the two currents by changing their weights (factors 1/10 and 1/5.09 in equations (1) and (2)). This modification was necessary to adapt the MEF model to the different AP mathematical description we used.

In order to close the loop (see Figure 1), the last point consisted in adding the two currents to the ODE of membrane potential: in this way the MEF was able to modulate the cellular electrical activity.

## 3. Results and Discussion

After completing the assemblage of the mathematical model, the first objective was validating its features.

As stated in the previous section, we decided to simulate ideal WLs. The work by Iribe et al. [6] is one of the few cases of experimental WL study on isolated cardiomyocytes in literature and it is based on a sequence of isometric and isotonic contractions/relaxations, which is in accordance to our setup. As shown in Figure 2, our model can reproduce experimental data for different length preloads (end-diastolic $L_m$) and force afterloads (end-systolic $F_m$). Due to the current impossibility to obtain reliable recordings of sarcomere length, only a qualitatively comparison between the two plots is possible, in fact x-axes refer to half sarcomere length in our simulation and to carbon fiber tip distance in experiments (see [6] for further information). However an important result is the slope of end-systolic Force-Length relation (ESFLR), which is constant and independent of preload and afterload values as in the experiments. Furthermore, a cellular equivalent of the classic Frank-Starling effect can be observed: an increase in length preload leads to an increased ability to perform work (see increased area of WLs in Figure 2).

A more comprehensive validation is given by Figure 3, in fact the model can also reproduce experimental WLs

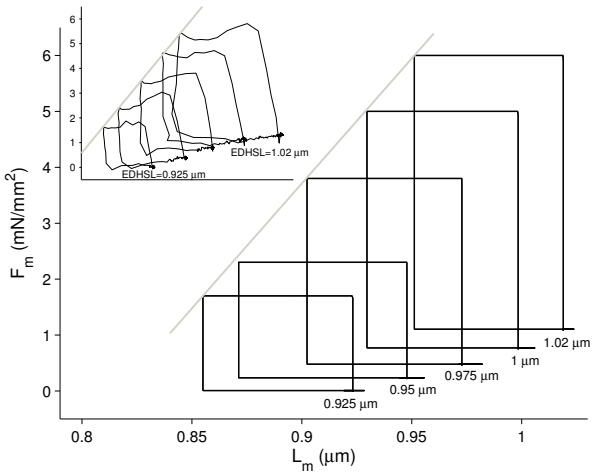


Figure 2. Comparison between simulated (main plot) and recorded (inset) WLs with varying end-diastolic $L_m$ (EDHSL 0.925 to 1.02 $\mu$m) and afterloads ($F_m$ 1.7 to 6 mN/mm$^2$). The grey straight lines represent the end-systolic Force-Length relations (ESFLRs) in simulations and experiments.

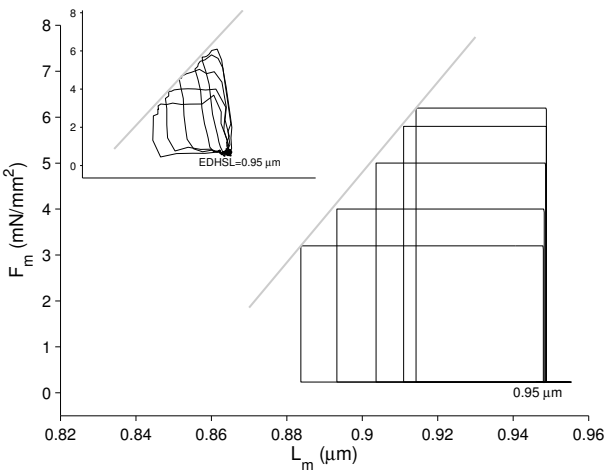


Figure 3. Comparison between simulated (main plot) and recorded (inset) WLs with constant end-diastolic $L_m$ (EDHSL 0.95 $\mu$m) and varying afterloads ($F_m$ 3.2 to 6.2 mN/mm$^2$). The grey straight lines represent the end-systolic Force-Length relations (ESFLRs) in simulations and experiments.

starting from a constant length preload but working against different force afterloads. As in the previous setup, ESFLR remains constant and independent of afterload values.

Figure 4 shows APs at different degrees of $\lambda$ as done by Gurev et al.. To obtain such traces equation (4) was substituted with constant values, so that the link between contraction and MEF blocks was interrupted. Our simulation results are in agreement with those of Gurev et al. and also with experimental results [7][8].

The validated model was used to investigate the role of MEF in modulating electrical activity during WL. We decided to employ the smallest WL (see Figure 2) because its variation of sarcomere length reflects that of in-vitro mammalian [9]. However simulations showed that results were in practice the same for every WL of our study.

The key point of the MEF effect on AP is represented by the strain sensed by the stretch-modulated currents, which depends on the resting half sarcomere length ($L_{m_o}$). As already mentioned, other simulation studies considered either constant values of stretch or conductance of the stretch-modulated channels, so that the role of $L_m$ and $L_{m_o}$ was ruled out. We analyzed the effect of different values of $L_{m_o}$, starting from $L_m$ during maximum contraction in the WL we employed (0.855 $\mu$m, see Figure 2) and reducing it until the MEF effect was saturated (0.60 $\mu$m), as shown in Figure 5.

Our simulations show that under basal conditions ($L_{m_o}$=0.855 $\mu$m, see Figure 5), MEF activation during the WL has a limited impact on AP. However, a progressive increase in the strain sensed by the stretch-modulated

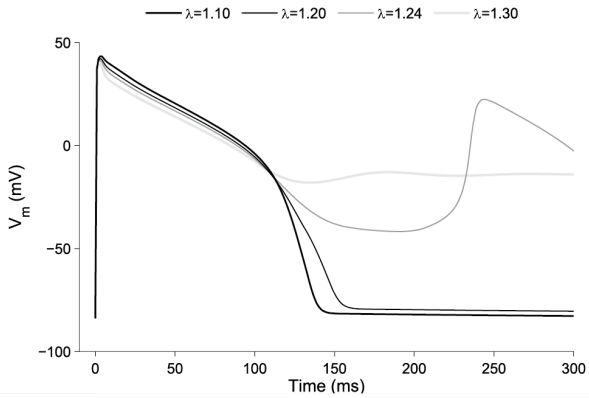


Figure 4. APs at different degrees of stretch ratio $\lambda$. See Figure 2B in [5] for a comparison.

currents, induced by decreasing $L_{m_o}$, results in DADs during fiber relaxation in AP phase 4 ($L_{m_o}$=0.75 $\mu$m), ectopic activations ($L_{m_o}$=0.70 $\mu$m) and triggered activity ($L_{m_o}$=0.68 $\mu$m).

## 4. Conclusions

Our complete mathematical description of mechanical and electrical ventricular myocyte activity is a useful tool to investigate MEF mechanisms, and its modular structure makes it able to provide further additional features, e.g. handling of $\beta$-adrenergic stimulation. The model successfully integrates cardiac cell electrophysiology and mechanics with physiological details such as ionic

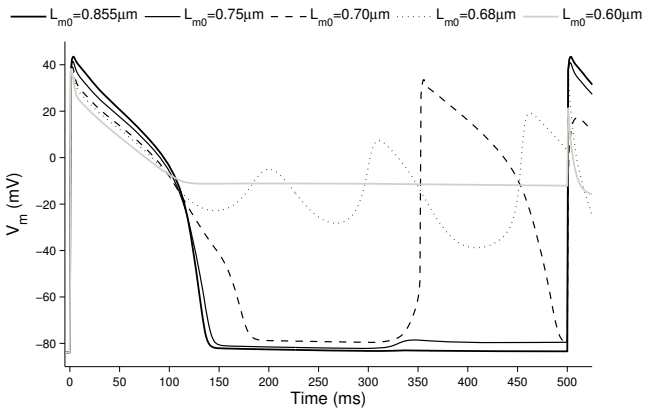


Figure 5. Time course of the transmembrane potential during application of a WL of 500ms duration at different levels of resting half sarcomere length ($L_{m_o}$).

membrane currents, intracellular $Ca^{2+}$ handling, cross-bridge formation and WL implementation. In real time, the electrical activity causes changes in the mechanical properties that in turn, depending on the cardiac phase active at the ongoing time step, affect the AP. In this way, it is also possible to analyze how a perturbation to the system propagates over time.

At the current stage the model can reproduce experimental WL and MEF studies [6][7][8], hence its utilization with the purpose of investigating the role of MEF in generating arrhythmogenic phenomena is fully justified. On the base of the preliminary simulation results, it can be speculated that the mentioned pathological behaviors could arise when the strength of the feedback is increased as under not-physiological or heavy exercise conditions, in which cardiac tissue is strongly stressed.

## Acknowledgements

This work was financially supported by a Hospal SpA grant (to SS) and a UK Medical Research Council Career Development award (to BR). The authors would like to thank Gentaro Iribe, Christian Bollensdorff and Peter Kohl for helpful discussions.

## References

[1] Kohl P, Sachs F, Franz MR. Cardiac Mechano-Electric Feedback and Arrhythmias: From Pipette to Patient. Philadelphia, PA: Elsevier, 2005.

[2] Kohl P, Bollensdorff C, Garny A. Effects of mechanosensitive ion channels on ventricular electrophysiology: experimental and theoretical models. Exp Physiol 2006;91:307–321.

[3] Negroni J, Lascano EC. Simulation of steady state and transient cardiac muscle response experiments with a huxley-based contraction model. Journal of Molecular and Cellular Cardiology 2008;45:300–312.

[4] Faber GM, Rudy Y. Action potential and contractility changes in $[Na^+]_i$ overloaded cardiac myocytes: a simulation study. Biophysical Journal 2000;78:2392–2404.

[5] Gurev V, Maleckar MM, Trayanova NA. Cardiac defibrillation and the role of mechanoelectric feedback in postshock arrhythmogenesis. Annal New York Academy of Sciences 2006;1080:320–333.

[6] Iribe G, Helmes M, Kohl P. Force-length relations in isolated intact cardiomyocytes subjected to dynamic changes in mechanical load. Am J Physiol Heart Circ Physiol 2007; 292:1487–1497.

[7] Isenberg G, Kazanski V, Kondratev D, Gallitelli MF, Kiseleva I, Kamkin A. Differential effects of stretch and compression on membrane currents and $[Na^+]_c$ in ventricular myocytes. Progress in Biophysics Molecular Biology 2003;82:43–56.

[8] Zabel M, Koller BS, Sachs F, Franz MR. Stretch-induced voltage changes in the isolated beating heart: importance of the timing of stretch and implications for stretch-activated ion channels. Cardiovascular Research 1996;32:120–130.

[9] Roos kP, Brady AJ. Individual sarcomere length determination from isolated cardiac cells using high-resolution optical microscopy and digital image processing. Biophys J 1982;40:233–244.

Address for correspondence:

Stefano Severi
Laboratorio di Ingegneria Biomedica
Universita' di Bologna
Via Venezia 52, 47521 Cesena, Italy
E-mail: stefano.severi@unibo.it